

Communication

Possible Wormhole Candidates in Active Galactic Nuclei

Mikhail Piotrovich , Serguei Krasnikov, Stanislava Buliga and Tinatin Natsvlishvili

Central astronomical observatory at Pulkovo, 196140 Saint-Petersburg, Russia; krasnikov.xxi@gmail.com (S.K.); aynim@yandex.ru (S.B.); tinatingao@mail.ru (T.N.)

* Correspondence: mpiotrovich@mail.ru

Received: 12 July 2020; Accepted: 9 August 2020; Published: 11 August 2020



Abstract: The hypothesis is considered that the active galactic nuclei (AGNs) are wormhole (WH) mouths rather than supermassive black holes (SMBHs). We study the difference in the physical properties of such objects from those of AGNs with SMBH, as well as the the corresponding difference in observational data. Firstly, the radiative efficiency for some types of WHs (both static and rotating) can be significantly larger than the theoretical maximal value for the Kerr SMBHs. A number of AGNs is presented, for which the observational data can be interpreted as the result of the presence of WHs in them. Secondly, a sufficiently strong gamma radiation with a characteristic spectrum noticeably differing from that of AGNs jets, can be emitted from a static WH as a result of a collision of accreting flows of matter inside the WH.

Keywords: active galactic nuclei; wormholes; accretion

1. Introduction

In recent years, an interesting hypothesis has been proposed that the active galactic nuclei (AGNs) in the centers of active galaxies are not supermassive black holes (SMBHs), but mouths of primordial macroscopic wormholes (WHs) [1–4]. This can lead to serious differences in the observational manifestations of such objects from AGNs with SMBHs.

2. Radiative Efficiency of AGNs with WHs

In considering AGNs, one uses such an important parameter as the radiative efficiency, defined as $\varepsilon = L_{bol} / \dot{M}c^2$, where L_{bol} is the bolometric luminosity of AGN, \dot{M} is the accretion rate, and c is the speed of light. In the case where the SMBH is located in the center of the AGN, ε in a special way depends on the spin (dimensionless angular momentum) of the SMBH $a_* = cJ / GM_{BH}^2$, where J is the angular momentum and M_{BH} is the mass of the SMBH [5]. Additionally, in particular, the maximum possible value is $\varepsilon \approx 0.324$ (at $a_* \approx 0.998$) [6].

It was shown in Harko et al. [7], Lobo [8] that, if, instead of the SMBH in the center of the AGN is placed a traversable, rotating WH of the Teo type [9], and the accretion in the form of a geometrically thin, optically thick accretion disk is considered, then the resulting picture will be quite different from the case of SMBH. For example, the radius of the innermost stable circular orbit R_{ISCO} , which, in the case of the SMBH, is highly sensitive to the spin and it varies within the range of $GM_{BH}/c^2 < R_{ISCO} < 6GM_{BH}/c^2$ (for $a_* \geq 0$) [5], in the case of WH, does not depend on the spin and it is equal to the radius r_{WH} of the mouth of the WH (for all wormholes in this paper we take $r_{WH} \approx 2GM_{WH}/c^2$). It is especially important that the radiative efficiency ε is also practically independent of spin and equal to about 0.5 (see Table 1 from Harko et al. [7]). It should be noted that this is a fairly significant difference, which is detectable in principle by the existing observational methods.

3. Estimations of Radiative Efficiency

We estimated the value of the radiative efficiency ε from observational data for a number of active galaxies. The list contains 112 Seyfert galaxies of the first, second and intermediate types, with the Eddington ratio $l_E = L_{bol}/L_{Edd}$ ($L_{Edd} = 1.5 \times 10^{38} M_{BH}/M_\odot$ is the Eddington luminosity) lying within the range of $0.01 < l_E < 0.3$, which allows for us to use a model of a geometrically thin, optically thick accretion disk.

The masses M_{BH} , the bolometric luminosities L_{bol} , and the angles between the normal to the plane of the accretion disk and the line of sight i were taken from Marin [10].

The estimations was carried out using six popular models that were taken from the literature.

1. Du et al. [11]: $\mu^{3/2}l_E = 0.201 \left(\frac{L_{5100}}{10^{44}}\right)^{1.5} M_8^{-2}\varepsilon(a)$.
2. Trakhtenbrot [12]: $\mu^{3/2}L_{bol} = 1.37 \times 10^{47} \left(\frac{\lambda L_\lambda}{10^{45}}\right)^{3/2} \left(\frac{\lambda}{5100}\right)^2 M_8^{-1}\varepsilon(a)$,
 $\lambda L_\lambda = L_{opt}, \lambda = 4400\text{\AA}$.
3. Davis and Laor [13]: $\mu^{3/2}L_{bol} = 1.48 \times 10^{47} \left(\frac{L_{opt}}{10^{45}}\right)^{1.5} M_8^{-1}\varepsilon(a)$.
4. Simple Newtonian accretion disk [13]:
 $\varepsilon(a) = 0.068 \left(\frac{L_{bol}}{10^{46}}\right) \left(\frac{L_{opt}}{10^{45}}\right)^{-3/2} M_8\mu^{3/2}$.
5. Raimundo et al. [14]: $\varepsilon(a) = 0.063 \left(\frac{L_{bol}}{10^{46}}\right)^{0.99} \left(\frac{L_{opt}}{10^{45}}\right)^{-1.5} M_8^{0.89}\mu^{3/2}$.
6. Lawther et al. [15]: $\mu^{3/2}L_{bol} = 0.87 \times 10^{47} \left(\frac{L_{opt}}{10^{45}}\right)^{1.5} \left(\frac{\lambda_{opt}}{4392}\right)^2 \varepsilon(a) M_8^{-1}$.

Definition of L_{opt} is taken from Hopkins et al. [16]:

$$\frac{L_{bol}}{L_{opt}} = \frac{L_{bol}}{L_B} = 6.25 \left(\frac{L_{bol}}{10^{10}L_\odot}\right)^{-0.37} + 9 \left(\frac{L_{bol}}{10^{10}L_\odot}\right)^{-0.012}, L_B = L(4400\text{\AA}), M_8 = \frac{M_{BH}}{10^8 M_\odot}.$$

$\mu = \cos i$, where i is the angle between the normal to the plane of the accretion disk and the line of sight.

Table 1 shows that, for our objects, most methods (and for some objects all methods) give ε values greater than 0.324—the maximal possible value for Kerr BH. Of course, this can be explained, for example, by erroneous determination of the magnitude of the bolometric luminosity or mass. However, the fact that there are a lot of such objects (about 7 % of the total list of 112 objects from [10]), as well as the fact that these objects are not distinguished by other parameters (distance, magnitude, mass, Eddington ratio etc.), speak in favor of the fact that this can be a real physical effect.

Table 1. The results of estimations of radiative efficiency for six popular models (see Section 3). Mass is expressed in $\log(M_{BH}/M_\odot)$, luminosity in $\log(L_{bol})$, L_{bol} in erg/s, i —in degrees, l_E —Eddington ratio.

Object	M_{BH}	i	L_{bol}	l_E	ε_1	ε_2	ε_3	ε_4	ε_5	ε_6
NGC 7213	$7.88^{+0.13}_{-0.18}$	21	44.3	$0.018^{+0.009}_{-0.004}$	$0.448^{+0.149}_{-0.149}$	$0.634^{+0.212}_{-0.210}$	$0.437^{+0.146}_{-0.145}$	$0.440^{+0.146}_{-0.146}$	$0.437^{+0.128}_{-0.132}$	$0.740^{+0.247}_{-0.245}$
PG 1302-102	$8.90^{+0.50}_{-0.50}$	32	46.33	$0.179^{+0.388}_{-0.122}$	$0.397^{+0.853}_{-0.272}$	$0.352^{+0.758}_{-0.241}$	$0.242^{+0.525}_{-0.165}$	$0.244^{+0.528}_{-0.167}$	$0.179^{+0.319}_{-0.115}$	$0.411^{+0.889}_{-0.281}$
Mrk 877	$8.79^{+0.15}_{-0.28}$	20	45.33	$0.023^{+0.021}_{-0.007}$	$1.140^{+0.460}_{-0.544}$	$1.190^{+0.490}_{-0.566}$	$0.819^{+0.341}_{-0.389}$	$0.824^{+0.336}_{-0.391}$	$0.635^{+0.228}_{-0.277}$	$1.390^{+0.570}_{-0.661}$
Mrk 6	$8.13^{+0.04}_{-0.43}$	26	44.56	$0.018^{+0.031}_{-0.001}$	$0.569^{+0.049}_{-0.360}$	$0.734^{+0.064}_{-0.464}$	$0.506^{+0.044}_{-0.320}$	$0.509^{+0.044}_{-0.322}$	$0.471^{+0.036}_{-0.277}$	$0.858^{+0.074}_{-0.542}$
UGC 3973	$7.85^{+0.15}_{-0.23}$	19	44.31	$0.019^{+0.014}_{-0.006}$	$0.426^{+0.175}_{-0.175}$	$0.601^{+0.248}_{-0.247}$	$0.414^{+0.171}_{-0.170}$	$0.417^{+0.171}_{-0.172}$	$0.417^{+0.150}_{-0.157}$	$0.702^{+0.289}_{-0.289}$
Mrk 1018	8.60	45	44.90	0.013	0.785	0.913	0.629	0.633	0.517	1.070
Mrk 1383	$8.97^{+0.12}_{-0.28}$	30	45.78	$0.043^{+0.039}_{-0.010}$	$0.906^{+0.284}_{-0.431}$	$0.870^{+0.280}_{-0.413}$	$0.600^{+0.190}_{-0.285}$	$0.603^{+0.193}_{-0.286}$	$0.440^{+0.122}_{-0.192}$	$1.020^{+0.320}_{-0.487}$
Mrk 876	$8.81^{+0.14}_{-0.21}$	27	45.81	$0.067^{+0.041}_{-0.018}$	$0.632^{+0.240}_{-0.243}$	$0.604^{+0.230}_{-0.232}$	$0.416^{+0.158}_{-0.159}$	$0.419^{+0.159}_{-0.161}$	$0.317^{+0.106}_{-0.111}$	$0.705^{+0.269}_{-0.270}$

4. High Energy Photons from Accretion on a Schwarzschild-like Wormholes

In this section, we show that the existence of traversable wormholes may lead to observable effects even if the former are of simplest non-rotating kind. To this end we consider a traversable wormhole connecting two galactic centers. To make the situation as simple as possible, assume that the wormhole is spherically symmetric, static, and empty everywhere beyond a spherical layer L . Assume further that the gravitational force acting on a radially falling test particle in any point of that wormhole is directed towards the throat. These properties make a wormhole very simple, but, at the same time, none of them look too unrealistic.

An example of a wormhole satisfying all listed requirements is a “Schwarzschild-like wormhole” [17]. Outside of the layer $L \equiv \{r < r_*\}$ this wormhole is empty and hence, by Birkhoff’s theorem, Schwarzschild’s (the corresponding mass will be denoted by M). r_* stands for some constant greater than (but close to) the throat’s radius.

The matter attracted by mouths of such a wormhole must form two fluxes colliding at the throat. The energy of the collision depends on the form of the wormhole and can, in principle, be arbitrarily high. Note that we are not challenging energy conservation: the collision is powered by the potential energy of the particles falling toward a gravitating body.

Consider, for example, a particle of mass μ that falls freely from infinity (with zero initial velocity) and in the throat of the wormhole hits head-on exactly the same oncoming particle. The energy—in the center-of-mass system—of such a collision is

$$E_{\text{c.m.}} \approx 2\mu\Gamma c^2, \quad \Gamma \equiv \max g_{00}^{-1/2}, \tag{1}$$

see Equation (12) in [17]. As a result, an external observer will see two spheres (these are the spheres—with radii r_* —bounding L) of ultra relativistic plasma. The said spheres radiate with a distinctive spectrum, see below, much different from those of jets or accretion disks, which makes it possible to identify the wormhole.

The phenomenon in discussion is rather complex and, to explore it, we will make as much simplifying assumptions as possible. Specifically, we consider a pair of AGNs with the masses $M \approx 4 \times 10^8 M_\odot$ connected by a Schwarzschild-like wormhole with $\Gamma \approx 10$. Assuming that

1. the galactics in question are Narrow-line Seyfert 1 Galaxies (NLS1) [18–22], they have a rather weak gamma radiation, thus, our supposed WH gamma radiation will be less diluted;
2. the plasma layer is heated (only) by the collision of the fluxes; and,
3. the magnetic field, the interaction of the infalling matter with the outcoming radiation, and the backreaction of the spheres on the metric of the wormhole are negligible.

we can write down the following rough estimates.

The characteristic accretion rates of NLS1 lie [23,24] within the range of $\dot{m} \approx (0.1 \div 1)M_\odot / 1 \text{ year}$, which means in our rough approximation

$$\dot{m} \approx 1M_\odot / 1 \text{ year}. \tag{2}$$

According to estimates of duty cycles of AGNs of type under consideration [25–27], this accretion regime should exist for at least 10^8 years. Accordingly, the mass of the plasma spherical layer is at least

$$m \approx 10^8 M_\odot, \tag{3}$$

where the layer’s mass m is understood as the integral of density rather than a characteristic of the wormhole’s metric. By (3), the proton concentration in the accreting plasma is

$$n_{\text{acc}} \approx M_\odot / (m_p 4\pi r_*^2 \cdot \sqrt{g_{*00}} \text{ ly}), \tag{4}$$

where m_p is the proton mass. Substituting our parameters in this expression we obtain the estimate

$$n_{acc} \approx 4 \frac{\Gamma}{(M/M_{\odot})^2} \cdot 10^{27} \text{ cm}^{-3}, \tag{5}$$

Finally, if we take an AGN mass to be $M \approx 4 \times 10^8 M_{\odot}$ and $\Gamma \approx 10$, then $n_{acc} \approx 10^{11} \text{ cm}^{-3}$.

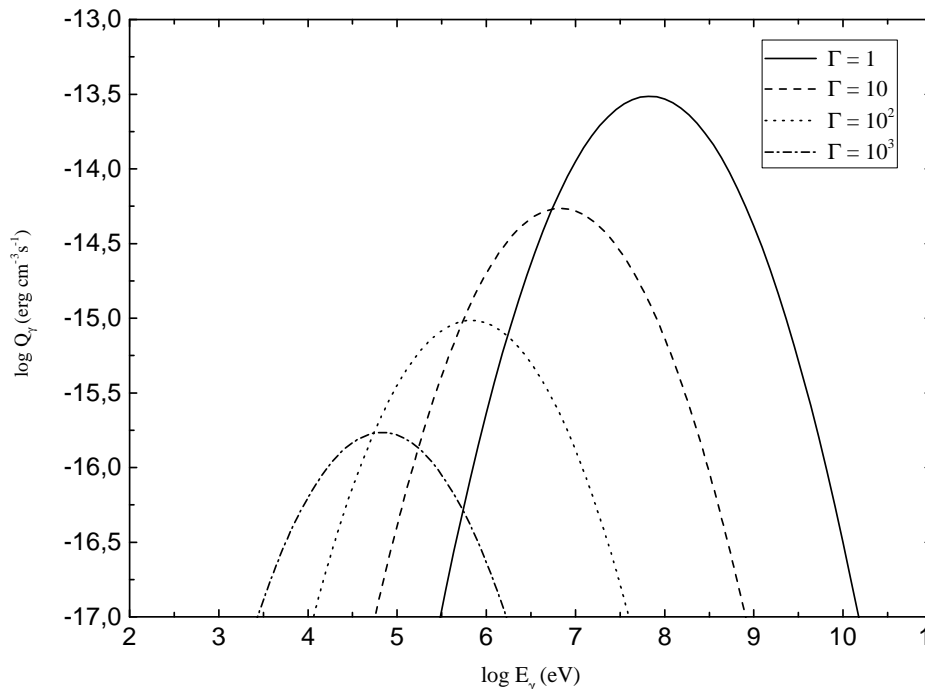


Figure 1. Gamma-ray production spectrum for ultrarelativistic plasma [28] taking into account the effects of the wormhole for different values of Γ .

On the other side, by Equation (1), the temperature T of the plasma cloud is approximately

$$T \approx \Gamma m_p c^2 / k \approx 10^{13} \Gamma \text{ K}, \tag{6}$$

where k is the Boltzmann constant.

The plasma with such a temperature and proton concentration was considered, for example, in Marscher et al. [28]; below, we will use their results. At high temperatures in the plasma the production of π^0 mesons begins [28–30]. π^0 mesons decay into two photons with energies $\sim 68 \text{ MeV}$. For $T = 2.5 \times 10^{13} \text{ K}$ and $T = 10^{14} \text{ K}$ the gamma-ray production spectra of plasma for this radiation mechanism (in Minkowski space) were found in Marscher et al. [28]. The latter spectrum has a peak value of $\log(Q_{\max}(\text{erg cm}^{-3} \text{ s}^{-1})) \approx 13.4$ at about 68 MeV , where Q is the gamma-ray production value. To find the spectrum of the wormhole (as measured by an observer resting out of the wormhole), we extrapolate Marscher’s result and assume that the peak value in the spectrum is reached at $\sim 68\Gamma^{-1} \text{ MeV}$ (the factor Γ^{-1} is due to the red shift experienced by a photon on its way from the throat to infinity) and it is equal to $\log(Q_{\max}(T)) \approx \log(Q_{\max}(T = 10^{14} \text{ K})) + 0.25 \log(T/10^{14} \text{ K}) - \log(\Gamma)$. The resulting spectrum looks (qualitatively), as shown in Figure 1.

The observed values of the flux from NLS1 is $\sim 10^{-13} \text{ erg cm}^{-2} \text{ s}^{-1}$ and the characteristic distance for observed AGNs of this type is about 10^9 light years. In order for the whole flux to be generated, the volume of the radiating plasma needs to be $\approx 10^{54} \text{ cm}^3$.

Further, in [28] the plasma is optically thin, so we consider radiation only from outer layers of plasma cloud with a volume of 10% of the total volume of cloud. Thus, the full cloud volume will be $\sim 10^{55} \text{ cm}^3$. Taking into account (5) we obtain the mass of the plasma cloud

$$m = n_{acc} m_p V \approx 10^8 M_{\odot} \tag{7}$$

When comparing this with (3), we see that the observed accretion rate (2) is sufficiently high for WH radiation to be observable.

5. Conclusions

Summing up we can conclude that:

1. Eight AGNs may contain WH instead of SMBH judging from their radiative efficiency.
2. A peak at about (0.1–10) MeV range may appear in the spectrum of an AGN with WH. This peak can be quite high, comparable to the observed radiation of NLS1.

Author Contributions: Conceptualization, M.P. and S.K.; methodology, M.P. and S.K.; validation, M.P. and S.K.; formal analysis, M.P., S.K., S.B. and T.N.; investigation, S.B. and T.N.; resources, S.B. and T.N.; data curation, S.B. and T.N.; writing—original draft preparation, M.P. and S.K.; writing—review and editing, M.P. and S.K.; visualization, M.P. and S.B.; supervision, M.P. and S.K.; project administration, M.P.; funding acquisition, S.K. All authors have read and agreed to the published version of the manuscript.

Funding: S.K. is grateful to RFBR for financial support under grant No. 18-02-00461 “Rotating black holes as the sources of particles with high energy”.

Acknowledgments: The authors are grateful to the reviewers for useful comments and advice.

Conflicts of Interest: The authors declare no conflict of interest.

References

1. Kardashev, N.S.; Novikov, I.D.; Shatskiy, A.A. Astrophysics of Wormholes. *Int. J. Mod. Phys.* **2007**, *16*, 909–926. [[CrossRef](#)]
2. Bambi, C. Can the supermassive objects at the centers of galaxies be traversable wormholes? The first test of strong gravity for mm/sub-mm very long baseline interferometry facilities. *Phys. Rev. D* **2013**, *87*, 107501. [[CrossRef](#)]
3. Li, Z.; Bambi, C. Distinguishing black holes and wormholes with orbiting hot spots. *Phys. Rev. D* **2014**, *90*, 024071. [[CrossRef](#)]
4. Zhou, M.; Cardenas-Avendano, A.; Bambi, C.; Kleihaus, B.; Kunz, J. Search for astrophysical rotating Ellis wormholes with x-ray reflection spectroscopy. *Phys. Rev. D* **2016**, *94*, 024036. [[CrossRef](#)]
5. Bardeen, J.M.; Press, W.H.; Teukolsky, S.A. Rotating Black Holes: Locally Nonrotating Frames, Energy Extraction, and Scalar Synchrotron Radiation. *Astrophys. J.* **1972**, *178*, 347–370. [[CrossRef](#)]
6. Thorne, K.S. Disk-Accretion onto a Black Hole. II. Evolution of the Hole. *Astrophys. J.* **1974**, *191*, 507–520. [[CrossRef](#)]
7. Harko, T.; Kovács, Z.; Lobo, F.S.N. Thin accretion disks in stationary axisymmetric wormhole spacetimes. *Phys. Rev. D* **2009**, *79*, 064001. [[CrossRef](#)]
8. Lobo, F.S.N. Wormholes, Warp Drives and Energy Conditions. *Fundam. Theor. Phys.* **2017**, *189*. [[CrossRef](#)]
9. Teo, E. Rotating traversable wormholes. *Phys. Rev. D* **1998**, *58*, 024014. [[CrossRef](#)]
10. Marin, F. Are there reliable methods to estimate the nuclear orientation of Seyfert galaxies? *Mon. Not. R. Astron. Soc.* **2016**, *460*, 3679–3705. [[CrossRef](#)]
11. Du, P.; Hu, C.; Lu, K.X.; Wang, F.; Qiu, J.; Li, Y.R.; Bai, J.M.; Kaspi, S.; Netzer, H.; Wang, J.M.; SEAMBH Collaboration. Supermassive Black Holes with High Accretion Rates in Active Galactic Nuclei. I. First Results from a New Reverberation Mapping Campaign. *Astrophys. J.* **2014**, *782*, 45. [[CrossRef](#)]
12. Trakhtenbrot, B. The Most Massive Active Black Holes at $z \sim 1.5$ – 3.5 have High Spins and Radiative Efficiencies. *Astrophys. J. Lett.* **2014**, *789*, L9. [[CrossRef](#)]
13. Davis, S.W.; Laor, A. The Radiative Efficiency of Accretion Flows in Individual Active Galactic Nuclei. *Astrophys. J.* **2011**, *728*, 98. [[CrossRef](#)]
14. Raimundo, S.I.; Fabian, A.C.; Vasudevan, R.V.; Gandhi, P.; Wu, J. Can we measure the accretion efficiency of active galactic nuclei? *Mon. Not. R. Astron. Soc.* **2012**, *419*, 2529–2544. [[CrossRef](#)]
15. Lawther, D.; Vestergaard, M.; Raimundo, S.; Grupe, D. A catalogue of optical to X-ray spectral energy distributions of $z \approx 2$ quasars observed with Swift—I. First results. *Mon. Not. R. Astron. Soc.* **2017**, *467*, 4674–4710. [[CrossRef](#)]

16. Hopkins, P.F.; Richards, G.T.; Hernquist, L. An Observational Determination of the Bolometric Quasar Luminosity Function. *Astrophys. J.* **2007**, *654*, 731–753. [[CrossRef](#)]
17. Krasnikov, S. Schwarzschild-like wormholes as accelerators. *Phys. Rev. D* **2018**, *98*, 104048. [[CrossRef](#)]
18. Paliya, V.S.; Parker, M.L.; Jiang, J.; Fabian, A.C.; Brenneman, L.; Ajello, M.; Hartmann, D. General Physical Properties of Gamma-Ray-emitting Narrow-line Seyfert 1 Galaxies. *Astrophys. J.* **2019**, *872*, 169. [[CrossRef](#)]
19. Kynoch, D.; Landt, H.; Ward, M.J.; Done, C.; Boisson, C.; Baloković, M.; Angelakis, E.; Myserlis, I. The relativistic jet of the γ -ray emitting narrow-line Seyfert 1 galaxy PKS J1222+0413. *Mon. Not. R. Astron. Soc.* **2019**, *487*, 181–197. [[CrossRef](#)]
20. Madejski, G.G.; Sikora, M. Gamma-Ray Observations of Active Galactic Nuclei. *Annu. Rev. Astron. Astrophys.* **2016**, *54*, 725–760. [[CrossRef](#)]
21. Baghmany, V.; Sahakyan, N. X-ray and γ -ray emissions from NLSy1 galaxies. *Int. J. Mod. Phys.* **2018**, *27*, 1844001. [[CrossRef](#)]
22. Hu, C.; Wang, J.M.; Ho, L.C.; Chen, Y.M.; Zhang, H.T.; Bian, W.H.; Xue, S.J. A Systematic Analysis of Fe II Emission in Quasars: Evidence for Inflow to the Central Black Hole. *Astrophys. J.* **2008**, *687*, 78–96. [[CrossRef](#)]
23. Bian, W.H.; Zhao, Y.H. Accretion Rates and the Accretion Efficiency in AGNs. *Publ. Astron. Soc. Jpn.* **2003**, *55*, 599–603. [[CrossRef](#)]
24. Collin, S.; Kawaguchi, T. Super-Eddington accretion rates in Narrow Line Seyfert 1 galaxies. *Astron. Astrophys.* **2004**, *426*, 797–808. [[CrossRef](#)]
25. Shankar, F.; Weinberg, D.H.; Miralda-Escudé, J. Accretion-driven evolution of black holes: Eddington ratios, duty cycles and active galaxy fractions. *Mon. Not. R. Astron. Soc.* **2013**, *428*, 421–446. [[CrossRef](#)]
26. Aversa, R.; Lapi, A.; de Zotti, G.; Shankar, F.; Danese, L. Black Hole and Galaxy Coevolution from Continuity Equation and Abundance Matching. *Astrophys. J.* **2015**, *810*, 74. [[CrossRef](#)]
27. Tucci, M.; Volonteri, M. Constraining supermassive black hole evolution through the continuity equation. *Astron. Astrophys.* **2017**, *600*, A64. [[CrossRef](#)]
28. Marscher, A.P.; Vestrand, W.T.; Scott, J.S. Neutrino, gamma-ray, electron, and positron production in an ultrarelativistic plasma. *Astrophys. J.* **1980**, *241*, 1166–1174. [[CrossRef](#)]
29. Kolykhalov, P.I.; Syunyaev, R.A. Gamma emission during spherically symmetric accretion onto black holes in binary stellar systems. *Sov. Astron.* **1979**, *23*, 189–192.
30. Dermer, C.D. Binary Collision Rates of Relativistic Thermal Plasmas. II. Spectra. *Astrophys. J.* **1986**, *307*, 47–59. [[CrossRef](#)]



© 2020 by the authors. Licensee MDPI, Basel, Switzerland. This article is an open access article distributed under the terms and conditions of the Creative Commons Attribution (CC BY) license (<http://creativecommons.org/licenses/by/4.0/>).